Korean J. Chem. Eng., 34(2), 305-313 (2017)
DOI: 10.1007/s11814-016-0277-1

pISSN: 0256-1115
eISSN: 1975-7220

Ni/La_2O_3-ZrO_2 catalyst for hydrogen production from steam reforming of acetic acid as a model compound of bio-oil

Ya-ping Xue*,,***,****, Chang-feng Yan*,**,***,****,†, Xiao-yong Zhao*,**,***,****, Shi-lin Huang*,**,***, and Chang-qing Guo*,**,***

*Guangzhou Institute of Energy Conversion, Chinese Academy of Sciences, Guangzhou 510640, China
**Key Laboratory of Renewable Energy, Chinese Academy of Sciences, Guangzhou 510640, China
***Guangdong Key Laboratory of New and Renewable Energy Research and Development, Guangzhou 510640, China
****University of Chinese Academy of Sciences, Beijing 100039, China
(*Received 28 June 2016 • accepted 6 October 2016*)

Abstract−Hydrogen production from steam reforming of acetic acid was investigated over Ni/La_2O_3-ZrO_2 catalyst. A series of Ni/La_2O_3-ZrO_2 catalysts were synthesized by sol-gel method coupled with wet impregnation, which was characterized by XRD, BET, TEM, EDS, TG, SEM and TPR. Catalytic activity of Ni/La_2O_3-ZrO_2 was evaluated by steam reforming of acetic acid at the temperature range of 550-750 °C. The tetragonal phase $La_{0.1}Zr_{0.9}O_{1.95}$ is formed through the doping of La_2O_3 into the ZrO_2 lattice and nickel species are highly dispersed on the support with high specific surface area. H_2 yield and CO_2 yield of Ni/La_2O_3-ZrO_2 catalyst with 15%wt Ni reaches 89.27% and 80.41% at 600 °C, respectively, which is attributed to high BET surface area and sufficient Ni active sites in strong interaction with the support. 15%wt Ni supported on La_2O_3-ZrO_2 catalyst maintains relatively stable catalytic activities for a period of 20 h.

Keywords: Hydrogen Production, Ni/La_2O_3-ZrO_2 Catalyst, Steam Reforming, Bio-oil, Acetic Acid

INTRODUCTION

Hydrogen is widely considered as a future transport fuel and clean energy carrier because of its cleanness and high gravimetric energy density. Nowadays, fossil fuels including natural gas, naphtha and coal are still main sources for hydrogen production [1]. With the depletion of fossil fuels and deterioration of environment from pollution, renewable resources for hydrogen production are of great interest, such as biomass, which is a renewable and CO_2 neutral clean resource. Hydrogen production from biomass includes two main thermal-chemical methods: direct gasification of biomass and steam reforming of bio-oil, which is produced by fast pyrolysis of biomass [2]. Bio-oil is higher gravimetric energy density than biomass, with easy storage and transportation in the application [3]. As a result, steam reforming of bio-oil is a promising and economical way to produce hydrogen. Bio-oil is a complicated mixture, including acids, aldehydes, alcohols, ketones and other oxygenate compounds with several inferior characteristics such as high viscosity, high oxygen and water content, low heating value, and low pH value [4,5]. Different compounds in bio-oil have distinct steam reforming reactivity. The different fractions can be applied more efficiently by the separation of bio-oil. Currently, column chromatography, solvent extraction, and distillation are main bio-oil separation methods [6]. Solvent extraction can achieve the enrichment of compounds with similar polarity and is one of the promising isolation methods of bio-oil. Among many solvents, water is a cheap and efficient solvent, which can separate bio-oil into water-soluble and water-insoluble phases. The bio-oil water-soluble phase is widely applied for steam reforming to produce hydrogen. To design efficient catalysts for steam reforming of bio-oil, model compounds of bio-oil like acetic acid, ethanol, acetone and ethylene are already in use [7]. Several studies have been reported for steam reforming of acetic acid, which is regarded as the main component and representative model compound of bio-oil [8-10]. Steam reforming of acetic acid can be described as the following reactions [11],

Steam reforming of acetic acid:

$$CH_3COOH \leftrightarrow 2H_2+2CO \qquad \Delta H_r^0=+213.4\ kJ/mol \qquad (1)$$

Water gas shift reaction:

$$CO+H_2O \leftrightarrow H_2+CO_2 \qquad \Delta H_r^0=-41.0\ kJ/mol \qquad (2)$$

The overall steam reforming of acetic acid is:

$$CH_3COOH+2H_2O \leftrightarrow 4H_2+2CO_2 \qquad \Delta H_r^0=+131.4\ kJ/mol \qquad (3)$$

The influence of noble metal and nickel on steam reforming of acetic acid has been persistently investigated. Noble metal catalysts show high activities and good stability in steam reforming of acetic acid but they are rather expensive [12]. Nickel-based catalysts are low cost and have high C-C bond and C-H breaking activity and are widely studied in steam reforming of acetic acid. The type and features of catalyst support (Al_2O_3, ZrO_2, CeO_2 and La_2O_3) also play an important role in steam reforming of acetic acid. Bimbela studied catalytic steam reforming of acetic acid over Ni/Al_2O_3 and the catalyst with moderate nickel content showed the best performance because of good nickel dispersion and its stabiliza-

†To whom correspondence should be addressed.
E-mail: yancf@ms.giec.ac.cn

tion in the reaction conditions [13]. Román Galdámez found that Ni/Al_2O_3 modified with lanthanum did not increase the H_2 yield in steam reforming of acetic acid. A high content of lanthanum in the Ni/Al_2O_3 could not favor metallic dispersion and Ni/Al_2O_3-La_2O_3 catalysts could be less reduced than the Ni/Al_2O_3 catalyst [14]. Medrano found that the addition of calcium as a promoter on the Ni/Al_2O_3 catalyst did not result in an improvement in reforming activity and stability under the experimental conditions [15]. Medrano further chose calcium and magnesium as promoters to modify the Ni/Al_2O_3 catalyst. The catalysts with the Mg/Al molar ratio of 0.26 showed the best performance, while calcium modified catalysts showed lower carbon conversion; The addition of calcium generated an NiO phase with less interaction with the support [16]. Bimbela prepared a series of Ni/Al coprecipitated catalysts modified with magnesium and copper and tested in the catalytic steam reforming of model compounds. Copper as a promoter would induce a decrease in the initial reforming activity and an enhancement of the catalyst stability because of the Ni dilution effect and resistance to the formation of encapsulating coke, respectively [17]. Wang studied catalytic reforming of the water-rich distillation fraction from crude bio-oil molecular distillation over Ni/Al_2O_3; A slow decrease in H_2 content in the outlet gas was observed after 11 h, which was caused by coke deposits [18]. Wang further reported catalytic reforming of phenol, acetic acid and hydroxyacetone over an Ni/Al_2O_3 catalyst. They found that the nano-Al_2O_3 acted as a more superior support and was beneficial in the formation of more active sites on the catalyst surface by compared with Ni/r-Al_2O_3 [19].

Coke formation and sintering of particles are two main reasons of the deactivation of Ni-based catalysts [20]. A proper support is needed to improve the activity and stability because it affects the dispersion and stability of active metal, changes the electronic distribution and may participate in the reaction [21,22]. ZrO_2 is regarded as a promising support since ZrO_2 has proper acidic/basic features. The features can enhance the accumulation of steam and carbon oxides on the surface to improve hydrogen yield and prevent carbon deposition [23]. At the same time, the rare earth metal oxide La_2O_3 can interact strongly with Ni active phase and enhance the interaction between Ni and support, which is beneficial to producing highly dispersed Ni species and avoiding particle coalescence [24,25]. La_2O_3 also improves the stability of the catalysts by resisting and removing carbon deposited from metallic surface [26,27]. Therefore, the support ZrO_2 modified by adding a certain amount of La_2O_3 is attractive and the mixture material may both have proper acidic/basic features and interaction with Ni active phase to prevent carbon deposition and avoid sintering of catalyst particles [28,29]. Moreover, oxygen vacancies may be created on the support La_2O_3 and ZrO_2 by forming a solid solution, which is good for improving the redox property of support [30]. The Ni/La_2O_3-ZrO_2 may be a promising catalyst for hydrogen production from steam reforming of acetic acid, but active sites, the interaction between Ni and supports and the structure-activity relationship need to be further explored.

In this paper, a series of Ni/La_2O_3-ZrO_2 with different Ni contents were prepared and evaluated in steam reforming reaction of acetic acid. The catalytic activities in the terms of H_2 selectivity and CO_2 selectivity were related to the structural and chemical properties of the catalysts, indicating the interaction between Ni and support La_2O_3-ZrO_2 played an important role on catalytic activities.

EXPERIMENTAL

1. Catalyst Preparation

The mesoporous La_2O_3-ZrO_2 support was prepared through a surfactant-directed sol-gel method by using hexadecyltrimethyl ammonium bromide (CTAB) as a template. First, tailored amounts of $ZrOCl_2{\cdot}8H_2O$ and $La(NO_3)_3{\cdot}6H_2O$ were dissolved into the water. Second, CTAB was dissolved into the water and the PH was adjusted to 10 by adding NH_4OH. The molar ratio of ($ZrOCl_2{\cdot}8H_2O$+ $La(NO_3)_3{\cdot}6H_2O$) and CTAB was 1.4. Finally, the aqueous solution of $ZrOCl_2{\cdot}8H_2O$ and $La(NO_3)_3{\cdot}6H_2O$ was added slowly to the aqueous solution of CTAB and NH_4OH and then kept for two hours under vigorous stirring at 60 °C. The white precipitate was filtered and washed with deionized water followed by ethanol, then dried at 100 °C for 12 h. Finally, the precursor of La_2O_3-ZrO_2 support (10 wt% of La_2O_3) was put into the muffle furnace to calcine for 4 h at 600 °C.

A series of Ni catalysts supported on La_2O_3-ZrO_2 were prepared via incipient wetness impregnation method. The mixtures were dried at 100 °C for 12 h, and then heated to 800 °C at a rate of 5 °C min^{-1} and calcined for 6 h. NiO/ La_2O_3-ZrO_2 obtained was pre-reduced at 800 °C in 5% H_2/Ar for 4 hours. Ni/La_2O_3-ZrO_2 catalysts with Ni loading of 5, 10, 15, 20 and 25 wt% were denoted as 5 Ni/La_2O_3-ZrO_2, 10 Ni/La_2O_3-ZrO_2, 15 Ni/La_2O_3-ZrO_2, 20 Ni/La_2O_3-ZrO_2 and 25 Ni/La_2O_3-ZrO_2, respectively.

2. Catalyst Characterization

XRD analysis was performed in PANalyticalX'Pert diffractometer (X'Pert PRO MPD, PW3040/60) with the 2θ ranging from 10° to 90° with Cu-Kα (λ=0.154060 nm) radiation (40 kV, 40 mA). N_2 adsorption-desorption tests were conducted in a Quantachrome Autosorb-1 instrument. Prior to measurement, the samples needed to be degassed at 250 °C for 12 hours. BET formula was used to calculate the surface area, and BJH method was applied to calculate the total pore volume and average pore size of catalysts. The morphology of catalyst was further characterized by transmission electron microscopy (TEM) on a JEM-2100 microscope followed by the energy dispersive spectrometer (EDS) analysis. H_2-TPR characterization of the catalysts was executed in the following process: 30 mg of a powder sample was placed in a U quartz tube and then heated to 1,000 °C at a rate of 10 °C/min in the atmosphere of 10 vol% H_2/Ar. The consumption of hydrogen was determined by a TCD detector. TG was performed in a thermal analyzer (STA409PC) to evaluate coke deposited during the reaction on reacted catalyst. The temperature was increased to 900 °C at a rate of 10 °C min^{-1} and air flow was maintained at 80 ml min^{-1}.

3. Catalyst Activity Tests

Steam reforming of acetic acid involved a bench-scale fixed-bed reactor at atmospheric pressure in the temperature range of 550-750 °C. Prior to the reforming reaction, 100 mg Ni/La_2O_3-ZrO_2 catalyst was placed into a quartz tube reactor and pre-reduced at 800 °C in situ in a 5 vol% H_2/Ar stream (120 ml min^{-1}) for 4 hours. In the experiment, H_2O and acetic acid with the molar ratio of

steam to HAc of 3 were vaporized in preheating zone and then fed into the reactor at a constant rate of 0.78 $g_{\text{-acetic acid}}\ h^{-1}$ by a peristaltic pump. A thermocouple was placed into the center of the catalyst bed to detect reforming reaction temperatures, and a digital temperature controller was used to control the actual reaction temperature. The gaseous products consisting of H_2, CO, CH_4 and CO_2 were analyzed online by the gas chromatograph (GC 7890II) equipped with a TCD detector and a TDX-01 column. After a reforming reaction of 2 hours, the collected liquid was detected by the gas chromatographs (GC 7890A) with a FID detector and a DB-FFAP column.

The stability of 15 Ni/La_2O_3-ZrO_2 catalyst was evaluated for 20 h at 600 °C, H_2O/HAc=3 and WHSV=7.8 g-acetic acid/g-cata·h^{-1}.

4. Data Analysis

The activity of Ni/La_2O_3-ZrO_2 in the steam reforming of acetic acid was measured by the acetic acid conversion and H_2, CO, CH_4 and CO_2 selectivity. The calculation formulas are given as follows:

$$\text{HAc conversion (\%)} = \frac{\text{the moles of HAc in the feed} - \text{the moles of HAc in the effluent}}{\text{the moles of HAc in the feed}} \times 100\%$$

$$\text{H}_2\text{ yield (\%)} = \frac{\text{the moles of H}_2\text{ produced}}{4 \times \text{the moles of HAc in the feed}} \times 100\%$$

$$\text{CX yield (\%)} = \frac{\text{the moles of CX produced}}{2 \times \text{the moles of HAc in the feed}} \times 100\%$$

Where CX is CO, CH_4 and CO_2, respectively.

RESULTS AND DISCUSSION

1. Catalytic Characterization

The XRD patterns obtained for calcined catalysts are shown in Fig. 1(a). For $15Ni/ZrO_2$, the peaks of ZrO_2 are detected at about 2θ of 28.25°, 31.51°, 34.20°, 50.13° and 59.94°, which represent the monoclinic structure of (111), (−111), (002), (200) and (−131) planes, respectively. For Ni/La_2O_3-ZrO_2, ZrO_2 monoclinic phase and La_2O_3 phaseare both not detected. La^{3+} may be incorporated into the ZrO_2 lattice and a solid solution is formed. The peaks of $La_{0.1}Zr_{0.9}O_{1.95}$ are found at about 2θ of 30.25°, 35.00°, 50.27° and 60.05° corresponding to the tetragonal structure of (111), (200), (220) and (311) planes, respectively. As the solid solution of ZrO_2 and La_2O_3 is formed, oxygen vacancies and lattice distortion are created because La^{3+} (0.106 nm) has lower valence and larger ionic

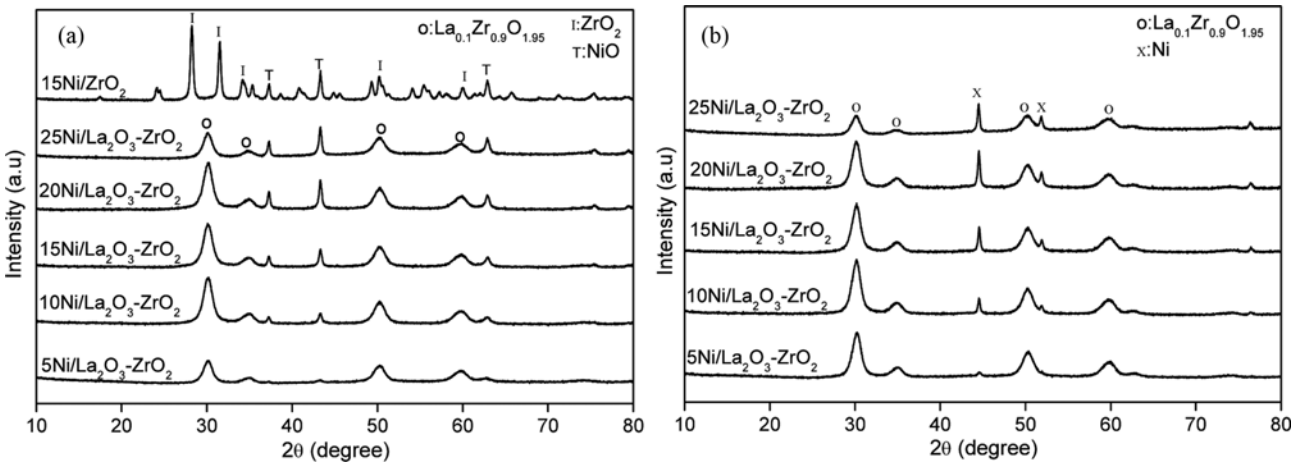

Fig. 1. XRD patterns of the calcined (a) and reduced (b) catalysts with different Ni content.

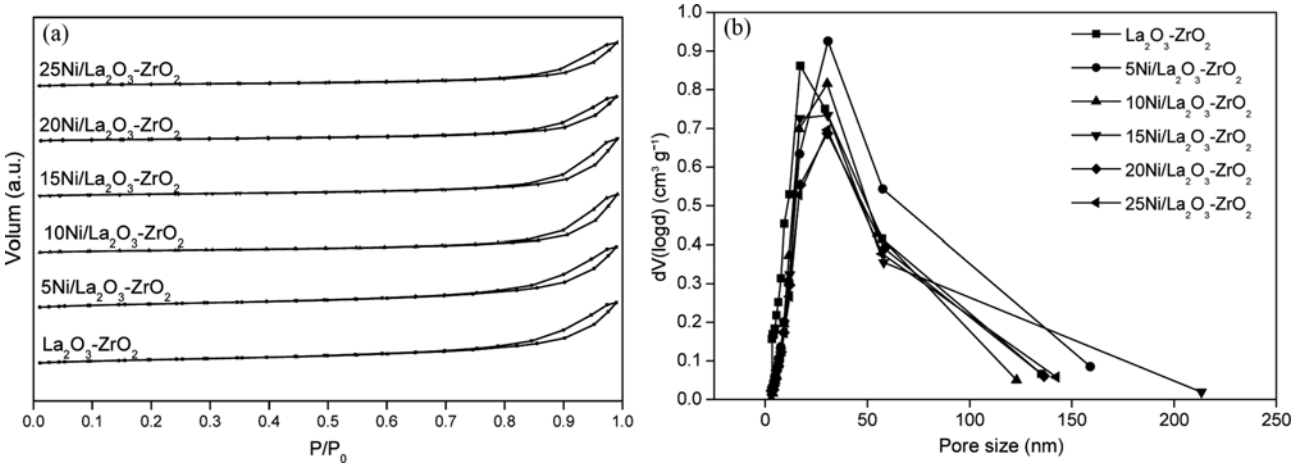

Fig. 2. N_2 physisorption isotherms (a) and pore size distribution curves (b) of reduced catalysts with different Ni content.

radius than the host ion Zr^{4+} (0.084 nm) [31]. The peaks of NiO phase are observed at 37.25°, 43.34° and 62.94°, which is attributed to the rhombohedral structure of (101), (012) and (104) planes, respectively. The XRD patterns of catalysts reduced at 800 °C for 4 h are shown in Fig. 1(b). Only the characteristic peaks of $La_{0.1}Zr_{0.9}O_{1.95}$ and Ni are identified for reduced catalysts, indicating NiO is completely reduced to Ni, which is the active site in steam reforming of acetic acid. And the peaks of Ni phase are observed at 44.49°, 51.86°, 76.36°, belonging to the cubic structure of (111), (002), (022) planes, respectively.

The adsorption-desorption isotherm obtained for La_2O_3-ZrO_2 support and Ni/La_2O_3-ZrO_2 catalysts shows type IV behavior with a well-developed hysteresis loop appearing in the relative pressure range from 0.7 to 1.0 as seen in Fig. 2. The hysteresis loop is not observed in low relative pressure region, indicating that all reduced catalysts possess large mesopores dimension [32,33]. Each curve shown in Fig. 2(b) has one narrow peak, suggesting that mesoporous Ni/La_2O_3-ZrO_2 has uniform pore dimension. As expected, the specific surface area of the La_2O_3-ZrO_2 support is high (176 m^2g^{-1}) prepared as listed in Table 1, which can result in homogeneous distribution of nickel particles and provide sufficient active adsorption sites for reactant molecules. With Ni content increasing, both the surface area and pore volume of Ni/La_2O_3-ZrO_2 gradually decrease, which possibly lies on the location of Ni particles inside the pores of La_2O_3-ZrO_2 and blockage of pores of supports. The pore size (nm) of Ni/La_2O_3-ZrO_2 decreases from 24.56 (Ni 5 wt%) to 22.90 (Ni 20 wt%) and increase from 22.90 (Ni 20 wt%) to 26.62 (Ni 25 wt%). 25 Ni/La_2O_3-ZrO_2 possesses largest average pore size because bigger pores (150-200 nm) occur based on Fig. 2(b).

To explore the morphology and structural characterization, 15 Ni/La_2O_3-ZrO_2 as a representative catalyst was further studied through HRTEM and electron diffraction pattern, and the interplanar spacing was obtained through Fourier transform as shown in Fig. 3. The pattern in Fig. 3(a) implies that the crystallite has

Table 1. Specific surface area and pore structure of catalyst with different Ni content

Ni/La_2O_3-ZrO_2 Ni (wt%)	BET surface area (m^2g^{-1})	Pore volume (cm^3g^{-1})	Pore size (nm)
0	176.31	0.71	16.01
5	108.40	0.67	24.56
10	95.20	0.58	24.21
15	92.54	0.53	23.06
20	89.39	0.51	22.90
25	74.41	0.49	26.62

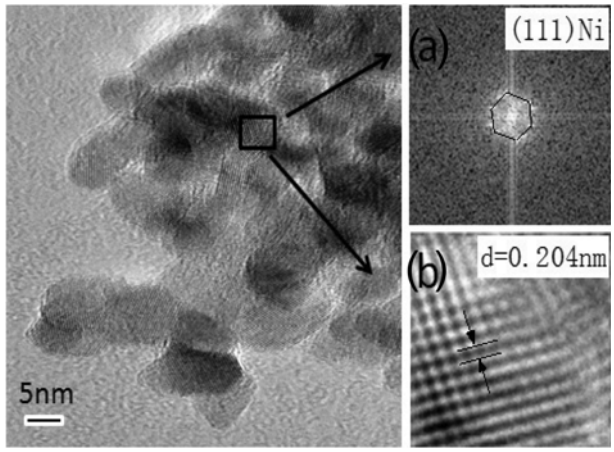

Fig. 3. HRTEM images of Ni/La_2O_3-ZrO_2 catalyst with 15%wt Ni.

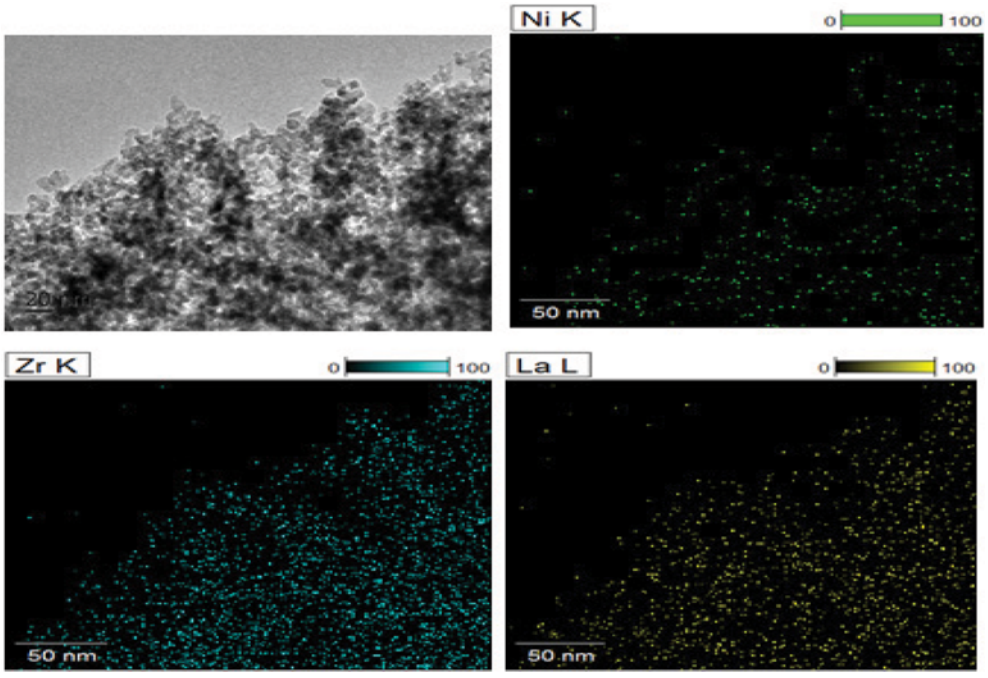

Fig. 4. HRTEM images of Ni/La_2O_3-ZrO_2 catalyst with 15% Ni.

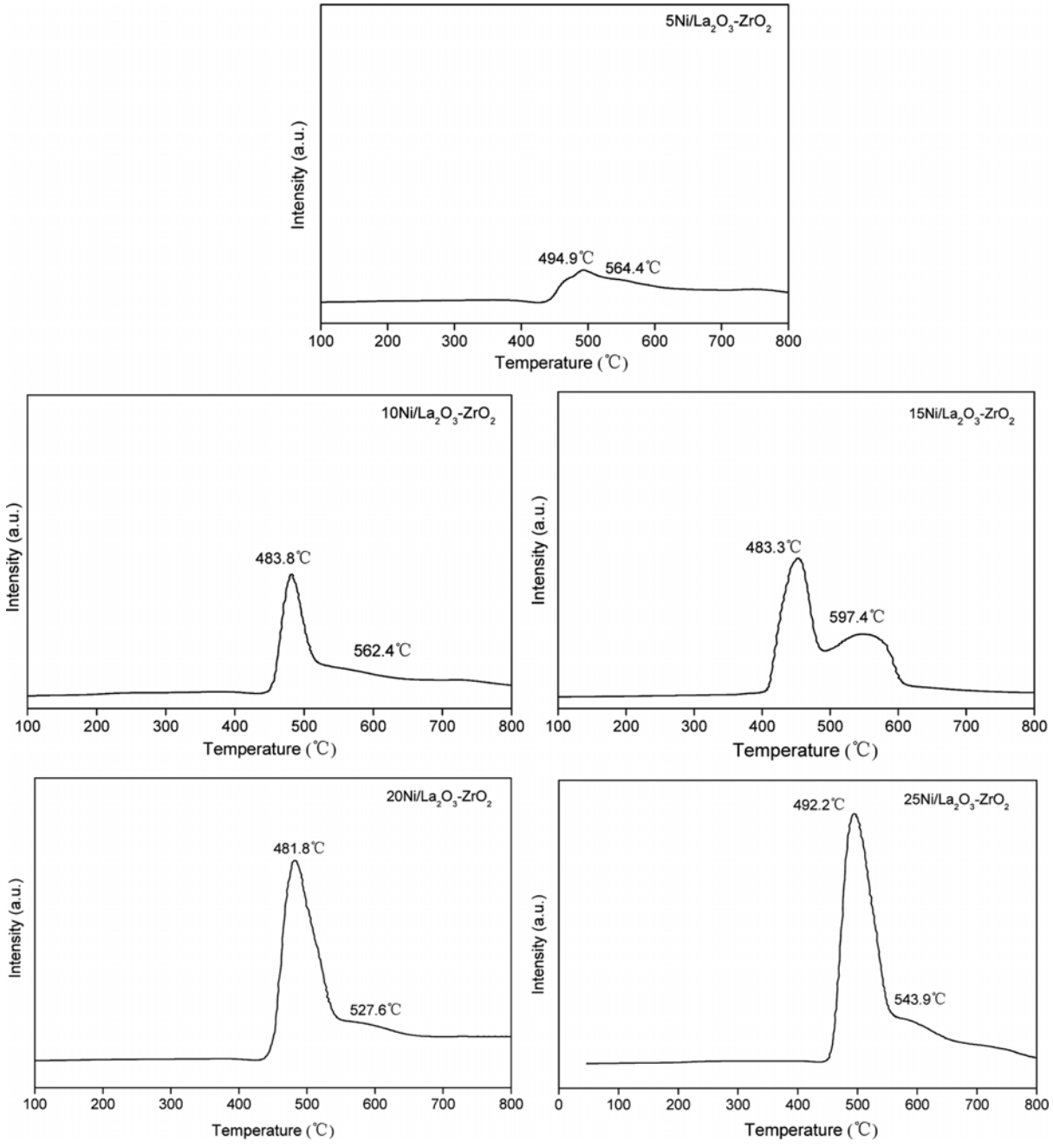

Fig. 5. H_2-TPR profiles of catalysts with different Ni content.

cubic or hexagonal structure. The crystallite corresponds to cubic nickel nanocrystal, mainly because XRD characterization shows that only cubic Ni and tetragonal $La_{0.1}ZrO_{0.9}O_{1.95}$ are detected. Moreover, the corresponding interplanar spacing of nickel (111) crystal is 0.204 nm, which is very close to the interplanar spacing of 0.203 nm obtained by XRD analysis. Based on the analysis of 54 particles, the particle size of Ni-based catalyst is determined as 4-12 nm. Ni species are highly dispersed on the support as shown in Fig. 4, probably due to the good interaction between Ni and support La_2O_3-ZrO_2 [34].

La_2O_3-ZrO_2 support is not reduced under 900 °C and only reduction peaks of NiO species are observed in Fig. 5. The peaks at low temperature (481-494 °C) are attributed to NiO with no or weak interaction with supports [35,36]. The peaks at high temperature (527-597 °C) are assigned to the NiO in strong interaction with support La_2O_3-ZrO_2 [37]. The interaction between Ni and La_2O_3-ZrO_2 can improve the dispersion of active component, change the active Ni electronic distribution and enhance the synergistic effect between Ni phase and the support, which has positive effects on the reforming reaction. The amount of H_2 consumption for first reduction peak increases with Ni loading. The phenomenon indicates that more Ni phases in no or weak interaction with the support are provided, as shown in Table 2. But the amount of H_2 consumption for the second peak shows a different trend. The

Table 2. Tmax and H_2 consumption (mmol gcat-1) of the TPR peaks obtained for the Ni/La_2O_3-ZrO_2 with different Ni content

Ni/La_2O_3-ZrO_2 Ni (wt%)	T_{max} (°C)		Hydrogen consumption (mmol g-cat^{-1})	
	1st peak	2nd peak	1st peak	2nd peak
5	492.2	543.9	0.42	0.43
10	481.8	527.6	0.92	0.59
15	483.3	597.4	1.19	1.18
20	483.8	562.4	2.49	0.84
25	494.9	564.4	2.98	0.87

amount of H_2 consumption (mmol g-cat^{-1}) for the second peak increases from 0.43 (Ni 5 wt%) to 1.18 (Ni 15 wt%) and decreases from 1.18 (Ni 15 wt%) to 0.87 (Ni 25 wt%). The 15 Ni/La_2O_3-ZrO_2 has the largest hydrogen consumption for the second peak among all the catalysts, indicating that the catalyst possesses the most Ni sites interacting strongly with La_2O_3-ZrO_2.

2. Catalytic Performance

Catalytic activity of Ni/La_2O_3-ZrO_2 catalysts was evaluated in steam reforming of acetic acid in the temperature range of 550-750 °C as shown in Fig. 6. The conversion of acetic acid is near 100% at the temperature range of 550-750 °C. The yield of the gaseous products (H_2, CO, CH_4 and CO_2) is low at 550 °C, mainly because of the occurrence of ketonization reaction ($2CH_3COOH \rightarrow CH_3COCH_3+CO_2+H_2O$) and the formation of carbon, whereas the formation of acetone is limited to traces and the formation of gaseous products (mainly H_2, CO and CO_2) becomes predominant, and the yield of CH_4 for all catalysts is lower than 4% when the reaction temperature is above 550 °C.

With the increasing of reaction temperature from 600 °C to 650 °C, H_2 and CO_2 yield both follow the order of 15Ni/La_2O_3-ZrO_2>20Ni/La_2O_3-ZrO_2>10Ni/La_2O_3-ZrO_2~5Ni/La_2O_3-ZrO_2, except that 25Ni/La_2O_3-ZrO_2 shows the lowest yield of H_2 at 650 °C, probably due to the aggregation of Ni particles and the blocking of the pores of support, which will reduce the access of reactants to the active sites. 15Ni/La_2O_3-ZrO_2 shows the best catalytic activity and the H_2 yield and CO_2 yield reaches 89.27% and 80.41% at 600 °C, respectively. Meanwhile, the yield of CO has contrary trends. The yield of H_2 and CO_2 for Ni/La_2O_3-ZrO_2 catalysts is consistent with the number of nickel sites in strong interaction with support La_2O_3-ZrO_2 based on the hydrogen consumption of Ni/La_2O_3-ZrO_2 in Table 2. The phenomenon means that Ni atoms strongly interacting with the support are the active sites and play a leading role on the steam reforming of acetic acid at low temperature of 600 °C and 650 °C. The strong interaction between active metal and support enhances the synergistic effect between Ni phase and the support, which further facilitates adsorption and dissociation of water and the formation of hydrogen. Moreover, the strong interaction between nickel and La_2O_3-ZrO_2 may improve the dispersion and stability of nickel phases, which maintains sufficient Ni-support

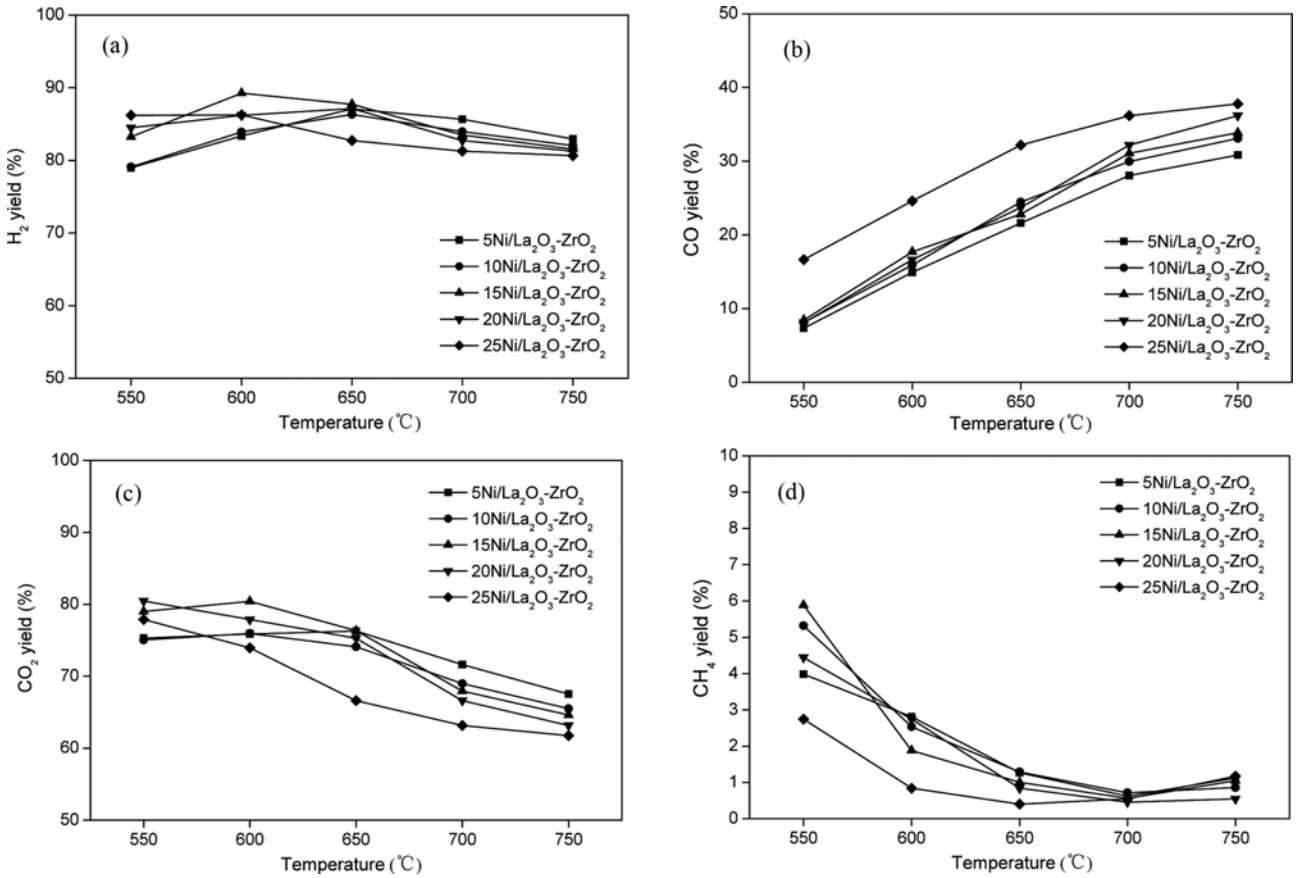

Fig. 6. The yield of gaseous products over Ni/La_2O_3-ZrO_2 in the temperature range of 550-750 °C.

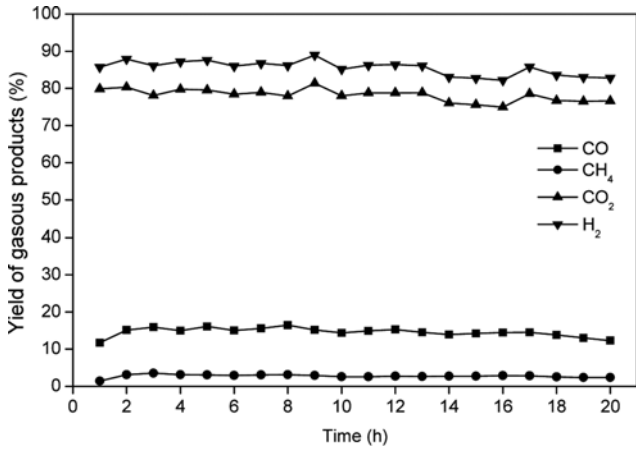

Fig. 7. The yield of gaseous products over 15Ni/La_2O_3-ZrO_2 for 20 h at 600 °C.

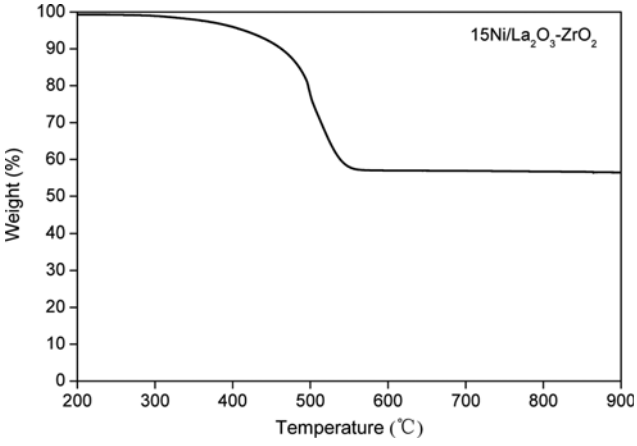

Fig. 10. TG image of 15Ni/La_2O_3-ZrO_2 after performing reforming reaction at 600 °C for 20 h.

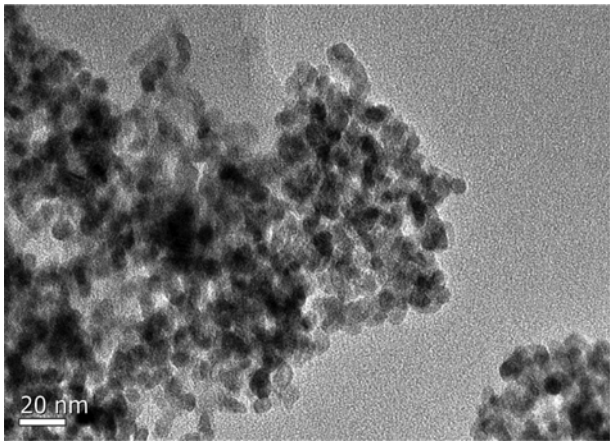

Fig. 8. HRTEM image of 15Ni/La_2O_3-ZrO_2 after performing reforming reaction at 600 °C for 20 h.

interfacial areas where the reaction may occur. With the increasing of reaction temperature from 700 °C to 750 °C, the H_2 yield and CO_2 yield decrease with increase of Ni contents. And the amount of Ni atoms in no or weak interaction with supports increases with Ni content increase in Table 2. The phenomenon indicates that the Ni phases in no or weak interaction with supports play a dominate role at high temperature, but they are not conducive to steam reforming of acetic acid.

3. Stability Test

A stability test of 15Ni/La_2O_3-ZrO_2 was conducted for 20 h at 600 °C, as shown in Fig. 7. The yield of H_2 for 15Ni/La_2O_3-ZrO_2 maintains above 82.78% within 20 h, indicating the material has high activity and good stability in the steam reforming of acetic acid. To investigate properties and structures of the catalyst after reforming reaction of 20 h, SEM, TG and TEM characterization were used to analyze the used catalyst. The TEM observation shows that the used catalyst particles have no obvious sintering as shown in Fig. 8. The SEM observation finds that filamentous carbon is formed by comparison to the reduced catalyst, but the catalyst still possesses rich porous structure on the surface and the nickel sites are not blocked. Fig. 10 shows that the amount of coke deposited on 15Ni/La_2O_3-ZrO_2 is 0.23 mmol $C \cdot h^{-1} \cdot g^{-1}_{\text{-acetic acid}}$ at 600 °C, which is lower than the amount of coke deposited on Ni/CeO_2-ZrO_2 and Ni/MgO-Al_2O_3 [38,36]. The amount of coke deposited on Ni/CeO_2-ZrO_2 and Ni/MgO-Al_2O_3 was 0.71 mmol$C \cdot h^{-1} \cdot g^{-1}_{\text{-acetic acid}}$ and 0.32 mmol$C \cdot h^{-1} \cdot g^{-1}_{\text{-acetic acid}}$, respectively. To know how good the performance was of Ni/La_2O_3-ZrO_2, the catalysts were compared with

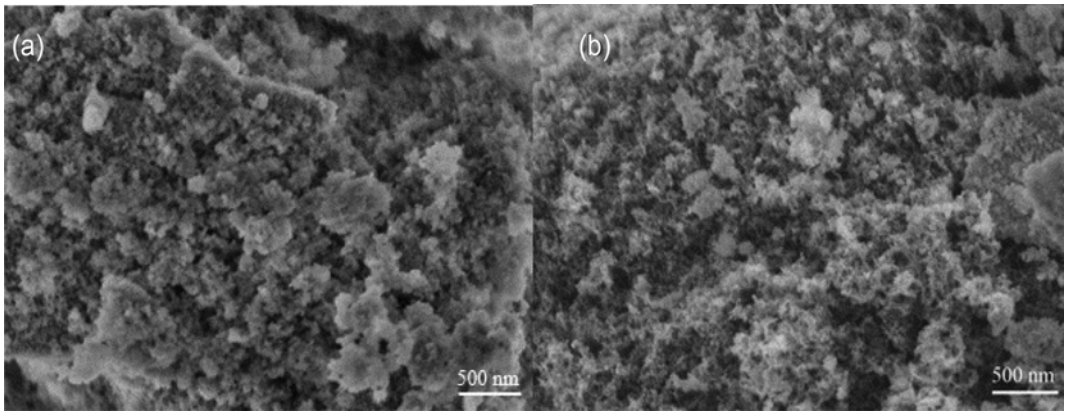

Fig. 9. SEM image of reduced 15Ni/La_2O_3-ZrO_2 (a) and 15Ni/La_2O_3-ZrO_2 after performing reforming reaction at 600 °C for 20 h (b).

Table 3. The H_2 yield and stability of catalysts in the steam reforming of acetic acid

Catalyst	Temperature (°C)	H_2O/HAc (mole/mole)	Y_{H2} (%)	Stability (h)	Reference
Ni/ZrO_2	500	2	74	3	[23]
Ni/Al_2O_3	600	3	61	4	[39]
Ni/CeO_2-ZrO_2	650	3	78	25	[8]
Ni/La_2O_3-Al_2O_3	600	5.7	20	---	[40]
Ni/MgO-Al_2O_3	600	2	69	20	[36]
Pd/HZM-5	600	18.4	60	--	[9]
Pt/ZrO_2	600	10	87	2	[41]
Co/La_2O_3-Al_2O_3	400	2	68	20	[27]
Ru/Mg(Al)O	700	6	70	20	[42]

similar catalyst system in the literature, as shown in Table 3. According to the characterization results, the superior performance of Ni/La_2O_3-ZrO_2 may be ascribed to high surface area, well-developed porosity and efficient Ni active sites. From this point, Ni/La_2O_3-ZrO_2 catalyst is one promising candidate for industrial application in the future.

CONCLUSION

Catalytic activity of Ni/La_2O_3-ZrO_2 with different Ni content was evaluated by steam reforming of acetic acid in the temperature range of 550-750 °C in a fixed-bed quartz reactor. $15Ni/La_2O_3$-ZrO_2 showed good catalytic activities and H_2 yield and CO_2 yield reached 89.27% and 80.41% at 600 °C. $15Ni/La_2O_3$-ZrO_2 catalyst maintained relatively stable catalytic activities for a period of 20 h. The results show that the tetragonal structure of $La_{0.1}Zr_{0.9}O_2$ phase is formed and the Ni/La_2O_3-ZrO_2 catalysts possess high surface area and uniform particle sizes. The Ni phases are the active sites in the reforming reaction, which are highly dispersed on the support. The interaction between Ni and support plays an important role in catalytic activities of the catalysts. Two types of Ni species were detected, which correspond to the Ni species in no interaction with supports and the Ni species strongly interacted with supports, respectively. The active Ni phase interacting with support La_2O_3-ZrO_2 plays a dominant role in catalytic activity at low temperature of 600 °C and 650 °C, whereas Ni with no or weak interaction with the support plays a leading role at high temperature.

ACKNOWLEDGEMENTS

The authors are grateful for the financial support of CAS Renewable Energy Key Lab., Natural Science Foundation of China (51576201), National Natural Science Foundation of Guangdong province (2015A030312007), Guangdong Science and Technology Project (2013B050800007), Guangzhou Science and Technology Project (2013J4500027).

REFERENCES

1. Y. Z. Lang, R. R. Arnepalli and A. A. Tiwari, *J. Nanosci. Nanotechnol.*, **11**, 3719 (2011).
2. N. L. Panwar, R. Kothari and V. V. Tyagi, *Renew. Sust. Energy Rev.*, **16**, 1801 (2012).
3. S. A. Chattanathan, S. Adhikari and N. Abdoulmoumine, *Renew. Sust. Energy Rev.*, **16**, 2366 (2012).
4. P. M. Mortensen, J. D. Grunwaldt, P. A. Jensen, K. G. Knudsen and A. D. Jensen, *Appl. Catal. A*, **407**, 1 (2011).
5. S. R. Wang, Y. R. Wang, Q. J. Cai, X. Y. Wang, H. Jin and Z. Y. Luo, *Sep. Purif. Technol.*, **122**, 248 (2014).
6. S. R. Wang, Q. J. Cai, X. Y. Wang, L. Zhang, Y. R. Wang and Z. Y. Luo, *Energy Fuels*, **28**, 115 (2014).
7. R. Trane, S. Dahl, M. S. Skjoth-Rasmussen and A. D. Jensen, *Int. J. Hydrogen Energy*, **37**, 6447 (2012).
8. X. X. Zheng, C. F. Yan, R. R. Hu, J. Li, H. Hai, W. M. Luo, C. Q. Guo, W. B. Li and Z. Y. Zhou, *Int. J. Hydrogen Energy*, **37**, 12987 (2012).
9. Q. Wang, S. R. Wang, X. B. Li and L. Guo, *Bioresources*, **8**, 2897 (2013).
10. A. C. Basagiannis and X. E. Verykios, *Appl. Catal. A-Gen.*, **308**, 182 (2006).
11. P. Mohanty, M. Patel and K. K. Pant, *Bioresour. Technol.*, **123**, 558 (2012).
12. T. Montini, L. DeRogatis, V. Gombac, P. Fornasiero and M. Graziani, *Appl. Catal. B-Environ.*, **71**, 125 (2007).
13. F. Bimbela, M. Oliva, J. Ruiz, L. García and J. Arauzo, *J. Anal. Appl. Pyrolysis*, **79**, 112 (2007).
14. J. Román Galdámez, L. García and R. Bilbao, *Energy Fuels*, **19**, 1133 (2005).
15. J. A. Medrano, M. Oliva, J. Ruiz, L. Garcia and J. Arauzo, *Int. J. Hydrogen Energy*, **33**, 4387 (2008).
16. J. A. Medrano, M. Oliva, J. Ruiz, L. García and J. Arauzo, *J. Anal. Appl. Pyrolysis*, **85**, 214 (2009).
17. F. Bimbela, D. Chen, J. Ruiz, L. Garcia and J. Arauzo, *Appl. Catal. B: Environ.*, **119-120**, 1 (2012).
18. S. R. Wang, X. B. Li, F. Zhang, Q. J. Cai, Y. R. Wang and Z. Y. Luo, *Int. J. Hydrogen Energy*, **38**, 16038 (2013).
19. S. R. Wang, Q. J. Cai, F. Zhang, X. B. Li, L. Zhang and Z. YLuo, *Int. J. Hydrogen Energy*, **39**, 18675 (2014).
20. J. L. Lu, B. S. Fu, M. C. Kung, G. M. Xiao, J. W. Elam, H. H. Kung and P. C. Stair, *Science*, **335**, 1205 (2012).
21. M. A. Khan and S. I. Woo, *Korean J. Chem. Eng.*, **31**, 1204 (2014).
22. H. J. Lee, G. S. Shin and Y. C. Kim, *Korean J. Chem. Eng.*, **32**, 1267 (2015).
23. Z. K. Li, X. Hu, L. J. Zhang, S. M. Liu and G. X. Lu, *Appl. Catal. a-*

Gen., **417**, 281 (2012).
24. H. Z. Feng, P. Q. Lan and S. F. Wu, *Int. J. Hydrogen Energy*, **37**, 14161 (2012).
25. G. Pantaleo, V. LaParola, F. Deganello, P. Calatozzo, R. Bal and A. M. Venezia, *Appl. Catal. B-Environ*., **164**, 135 (2015).
26. B. M. Guell, I. M. T. da Silva, K. Seshan and L. Lefferts, *Appl. Catal. B-Environ*., **88**, 59 (2009).
27. X. Hu and G. X. Lu, *Catal. Commun.*, **12**, 50 (2010).
28. S. H. Park, B. H. Chun and S. H. Kim, *Korean J. Chem. Eng*., **28**, 402 (2011).
29. W. Tao, G. W. Cheng, W. L. Yao, X. G. Lu, Q. H. Zhu, G. S. Li and Z. F. Zhou, *Int. J. Hydrogen Energy*, **39**, 18650 (2014).
30. T. F. Hou, B. Yu, S. Y. Zhang, J. H. Zhang, D. Z. Wang, T. K. Xu, L. Cui and W. J. Cai, *Appl. Catal. B-Environ*., **168**, 524 (2015).
31. Y. Z. Chen, B. J. Liaw, C. F. Kao and J. C. Kuo, *Appl. Catal. A-Gen*., **217**, 23 (2001).
32. A. Rumplecker, F. Kleitz, E. L. Salabas and F. Schuth, *Chem. Mater*., **19**, 485 (2007).
33. M. M. Nair, S. Kaliaguine and F. Kleitz, *Acs Catal.*, **4**, 3837 (2014).
34. G. Wu, C. Zhang, S. Li, Z. Huang, S. Yan, S. Wang, X. Ma and J. Gong, *Energy Environ. Sci*., **5**, 8942 (2012).
35. C. Jimenez-Gonzalez, Z. Boukha, B. de Rivas, J. J. Delgado, M. A. Cauqui, J. R. Gonzalez-Velasco, J. I. Gutierrez-Ortiz and R. Lopez-Fonseca, *Appl. Catal. A-Gen*., **466**, 9 (2013).
36. F. G. E. Nogueira, P. G. M. Assaf, H. W. P. Carvalho and E. M. Assaf, *Appl. Catal. B-Environ*., **160**, 188 (2014).
37. H. S. Roh, K. W. Jun, W. S. Dong, J. S. Chang, S. E. Park and Y. I. Joe, *J. Mol. Catal. A-Chem*., **181**, 137 (2002).
38. R. R. Hu, C. F. Yan, X. X. Zheng, H. Liu and Z. Y. Zhou, *Int. J. Hydrogen Energy*, **38**, 6033 (2013).
39. P. G. M. Assaf, F. G. E. Nogueira and E. M. Assaf, *Catal. Today*, **213**, 2 (2013).
40. K. K. Pant, P. Mohanty, S. Agarwal and A. K. Dalai, *Catal. Today*, **207**, 36 (2013).
41. K. Takanabe, K. Aika, K. Seshan and L. Lefferts, *Chem. Eng. J*., **120**, 133 (2006).
42. F. Bossola, C. Evangelisti, M. Allieta, R. Psaro, S. Recchia and V. Dal Santo, *Appl. Catal. B-Environ*., **181**, 599 (2016).